Cortico-Striatal Connections Predict Control over Speed and Accuracy in Perceptual Decision Making

Birte U. Forstmann[1,*], Andreas Schäfer[2], Alfred Anwander[2], Jane Neumann[2], Scott Brown[3], Eric-Jan Wagenmakers[1], Rafal Bogacz[4], Robert Turner[2]

Supplementary Online Material

Manual Segmentation of the Subthalamic Nucleus and Inter-rater Reliability

Manual segmentation was performed using the FSL 4.1.4 viewer. Segmentation was carried out by two independent researchers and inter-rater agreement was assessed. Only voxels rated by both raters as belonging to the STN were included in any further analysis. The manual segmentation was done as follows: In an initial step, the individual volumes obtained with the three different echoes of the GRE sequence were loaded into the viewer. This was done separately for each participant. Second, the contrast values in the viewer for the three different images were set to maximally increase visibility of the STN. Third, the coronal view was singled out and zoomed in to facilitate the drawing of the STN mask.

The human STN has a lens-shape form [1]. It borders and is surrounded by anatomical structures which served as additional landmarks to delineate the STN: (1) the substantia nigra pars compacta and pars reticularis with its caudal extension; the STN over-roofs the substantia nigra, (2) the red nucleus which is located in rostral direction.

Both the substantia nigra and red nucleus contain iron yielding a hypointense signal in T2-weighted images (GRE sequence) and are therefore easily discernable [1]. It should be noted that – in contrast to the rat STN for instance – the human STN is a closed nucleus [2]. Nonetheless, there is no clearly visible border between the anterior medial part of the STN and substantia nigra, and special precaution must be taken during manual segmentation. Inter-rater reliability coefficients are a crucial measure for this matter, but they do not rule out that the volume estimates of the STN might be slightly compromised.

Inter-rater reliability for the manual segmentation was assessed using the intra-class correlation coefficient (ICC) for brain volume [3] and Cohen's kappa [4], a statistical measure of inter-rater agreement for qualitative items. While ICC provides a measure for agreement between the raters across all segmentations of the same structure (i.e. left or right STN), Cohen's kappa is used to assess inter-rater agreement for every segmentation individually. Across subjects and hemispheres, Cohen's kappa varied between 0.74 and 0.93 with mean 0.86 (SD = 0.05). ICC for absolute agreement between raters with respect to the volume of the segmented structure was 0.94. Inter-rater agreement was additionally assessed by calculating the extent of overlap between the structures obtained by the two raters. This was done by superimposing the segmentation result from the second rater over the first, and determining the proportion of shared voxels by percent overlap = $Vox\_1 \cap Vox\_2 / Vox\_1$, where Vox_1 and Vox_2 contain all voxels regarded as part of the segmented structure by rater 1 and 2, respectively. Across subjects and hemispheres, the mean (SD) percent overlap was 0.87 (0.04). Finally, the STN masks were registered on the T1 images. A group overlap map of the STN masks was produced by normalization of the corresponding T1 weighted images.

Cortical and Subcortical Target Regions

A priori masks were chosen to compute the connectivity of areas within the cortico-basal ganglia network (**Fig. S1**). Except for the STN, the masks were taken from the Harvard-Oxford structural atlas as well as the Juelich histological atlas implemented in FSL. We estimated the strengths of connections between several regions chosen on the basis of the anatomical and neurocomputational hypotheses. In particular, we estimated the strength of connection between pre-SMA and striatum, as these connections were proposed to mediate control over SAT by the striatal hypothesis [5]. We also estimated the strength of connections between four cortical regions displayed in **Fig. S1 and S2** and STN (**Tables S1-S4**). These four regions were chosen for the following reasons: (i) Anterior cingulate cortex – its projections to STN have been originally proposed to mediate control over SAT [6]; (ii) Right inferior frontal gyrus – its projections to STN have been shown to mediate stopping of action execution [7,8]; (iii) Pre-SMA – it was found to modulate its activity with speed emphasis in all imaging studies of SAT [5, 9,10]; (iv) Primary motor cortex – it sends strong projections to STN [11]. **Fig. S3, S4, and S5** show the correlation (with 95% confidence intervals) between the tract strengths and the LBA measure of flexibility.

Independent Replication Study

We sought to replicate the results described above in an independent study. Twelve young subjects (8 females, mean age = 25.25, SD age = 3.47) underwent MRI scans on 3T Magnetom Trio scanner (Siemens, Erlangen) equipped with an 8-channel head array coil. The scan protocol was the same as described above with the exception of a change in the voxel resolution to 1.7 mm. Subjects also underwent behavioral testing with a moving-dot task as described in [5] and these data were again modeled with the LBA model, yielding an excellent fit with only LBA caution free to vary between speed and accuracy conditions. For the computation of probabilistic tractography, the same cortical and subcortical masks were used. For the probabilistic tracking between the cortical regions and the STN, averaged conjunction masks of the STN derived from the present study were used. Visual inspection ensured that the registration was correct.

The results corroborate the present findings in that only the tract strength between right pre-SMA and right striatum is predicted by the efficiency with which participants change their response thresholds. **Fig. S6, S7, and S8** show the correlation (with 95% confidence intervals) between the tract strengths (**Tables S4-S8**) and the LBA measure of flexibility. Note that the lack of association between LBA threshold flexibility and STN connectivity measures could in principle be due in part to the fact that we used the masks from the first study; nevertheless, the current procedure likely improves on current standards.

Model Specificity

In order to study the extent to which our results generalize across different behavioral models, we also applied the diffusion model [12] to the behavioral data. In the diffusion model, one parameter (i.e., boundary separation) quantifies response caution. Unfortunately, the diffusion model did not provide a parsimonious account of the data; that is, the experimental manipulation of speed vs. accuracy instructions did not selectively influence the boundary separation parameter, but also influenced drift rate (i.e., the quality of information processing) and non-decision processes. When we ignored the effects of the experimental manipulation on drift rate and non-decision time, the response caution parameter did not correlate with tract strength measurements (whereas the LBA parameter for response caution did). The failure to find a correlation could have been caused by excess sampling variability in the diffusion model parameter estimates, or it could have been the result of focusing only on the response caution parameter, when selective influence did not hold. For these data, therefore, we feel that both parameter selectivity and the ability to yield consistent results in an independent replication study argue that the LBA is the simpler and more appropriate model for the present application.

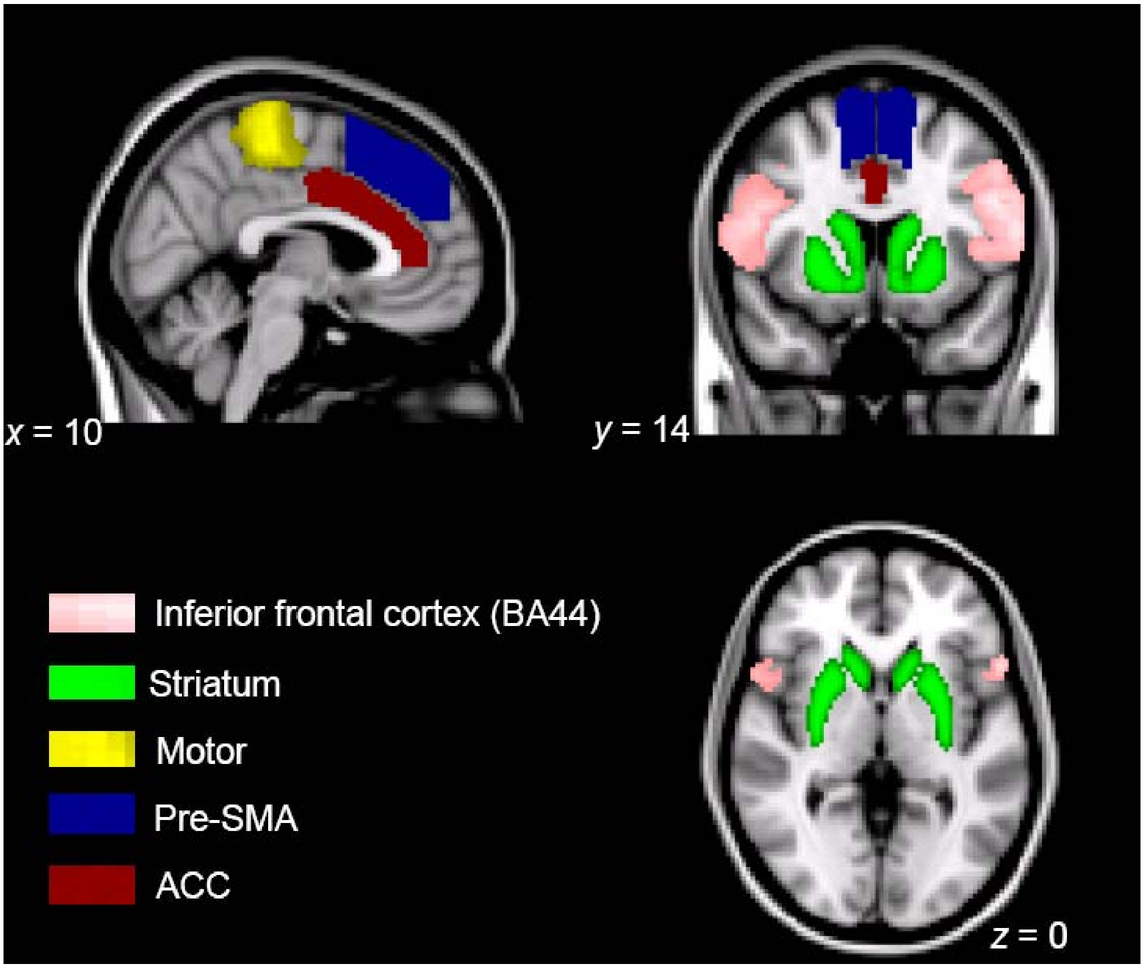

Figure S1. Location of brain areas for which connectivity was quantified.

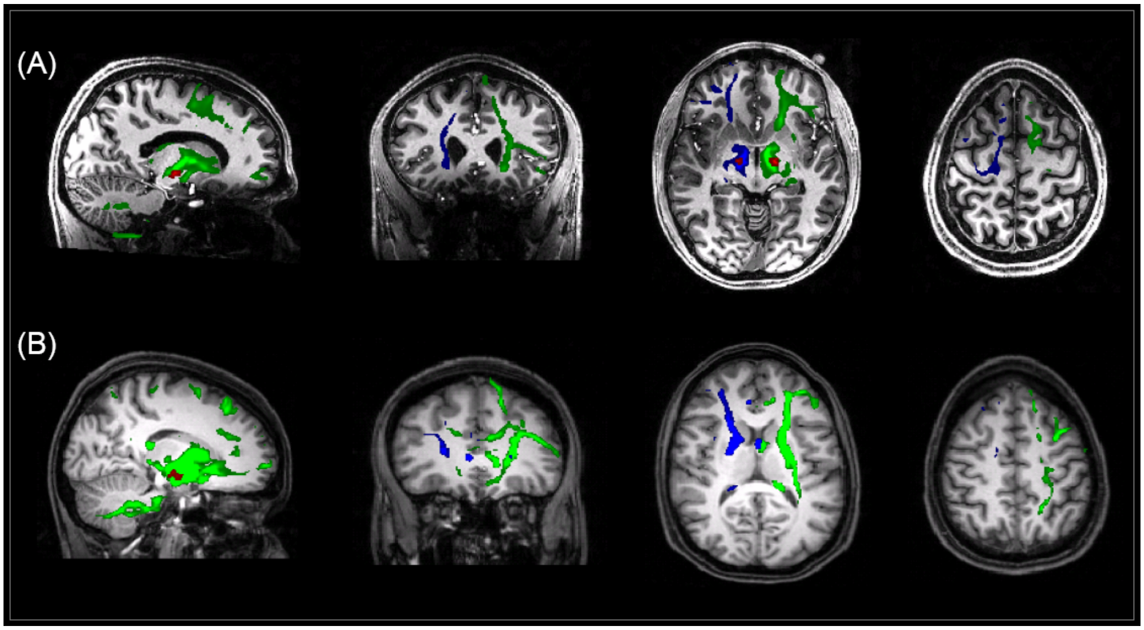

Figure S2. A) Reconstructed pathways from the mean conjunction masks (in red) of the left STN (blue pathways) and right STN (green pathways) into cortex from the main study. B) Reconstructed pathways from the mean conjunction masks (in red) of the left STN (blue pathways) and right STN (green pathways) into cortex from the replication study.

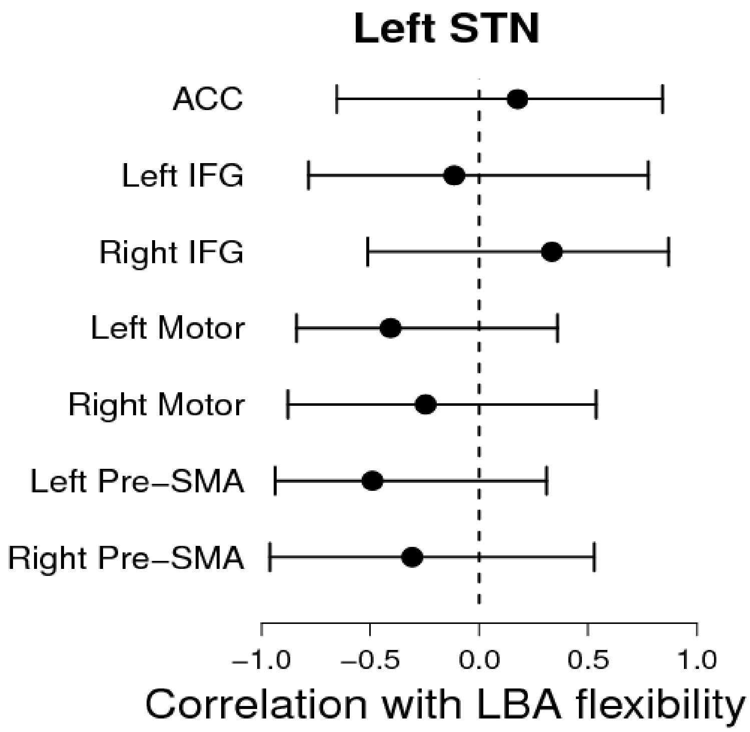

Figure S3. Correlation between LBA flexibility (i.e., the difference in the LBA caution parameter between accuracy and speed conditions) and tract strength from left STN to select brain areas. ACC = anterior cingulate cortex, IFG = inferior frontal gyrus (BA 44), pre-SMA = pre-supplementary motor cortex. Error bars indicate 95% confidence intervals.

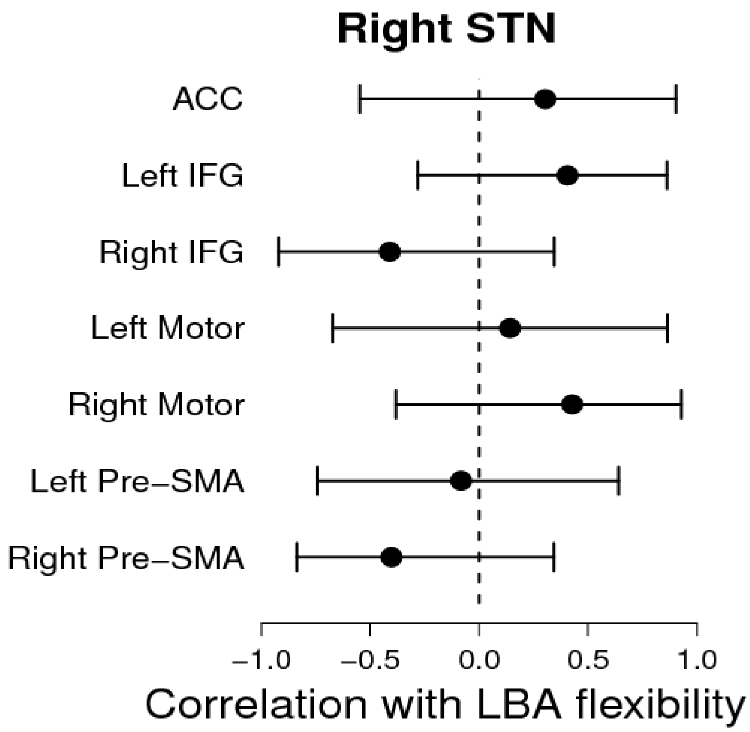

Figure S4. Correlation between LBA flexibility (i.e., the difference in the LBA caution parameter between accuracy and speed conditions) and tract strength from right STN to select brain areas. ACC = anterior cingulate cortex, IFG = inferior frontal gyrus (BA 44), pre-SMA = pre-supplementary motor cortex. Error bars indicate 95% confidence intervals.

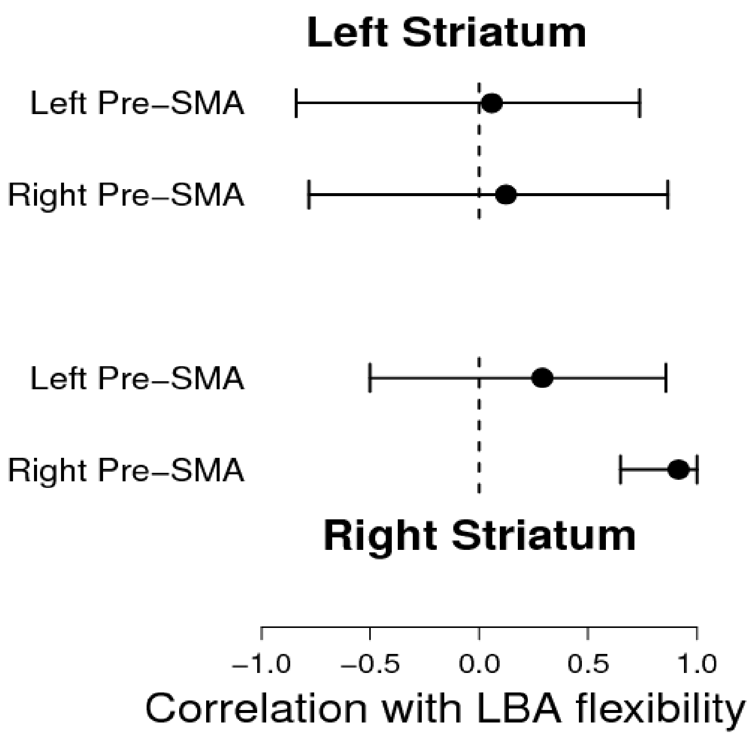

Figure S5. Correlation between LBA flexibility (i.e., the difference in the LBA caution parameter between accuracy and speed conditions) and tract strength from left and right striatum to left and right pre-SMA (i.e., pre-supplementary motor cortex). Error bars indicate 95% confidence intervals.

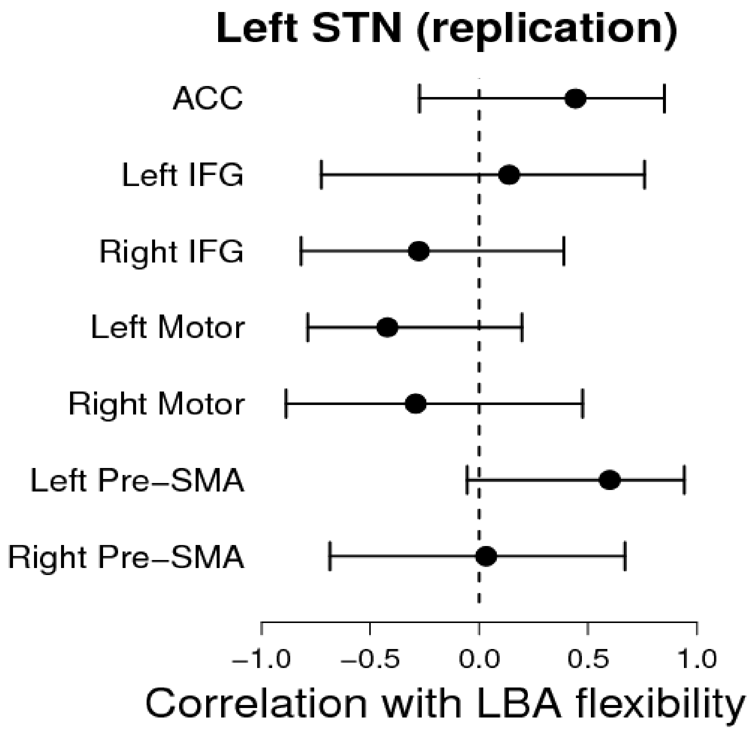

Figure S6. Correlation between LBA flexibility (i.e., the difference in the LBA caution parameter between accuracy and speed conditions) and tract strength from left STN to select brain areas (for the replication study). ACC = anterior cingulate cortex, IFG = inferior frontal gyrus (BA 44), pre-SMA = pre-supplementary motor cortex. Error bars indicate 95% confidence intervals.

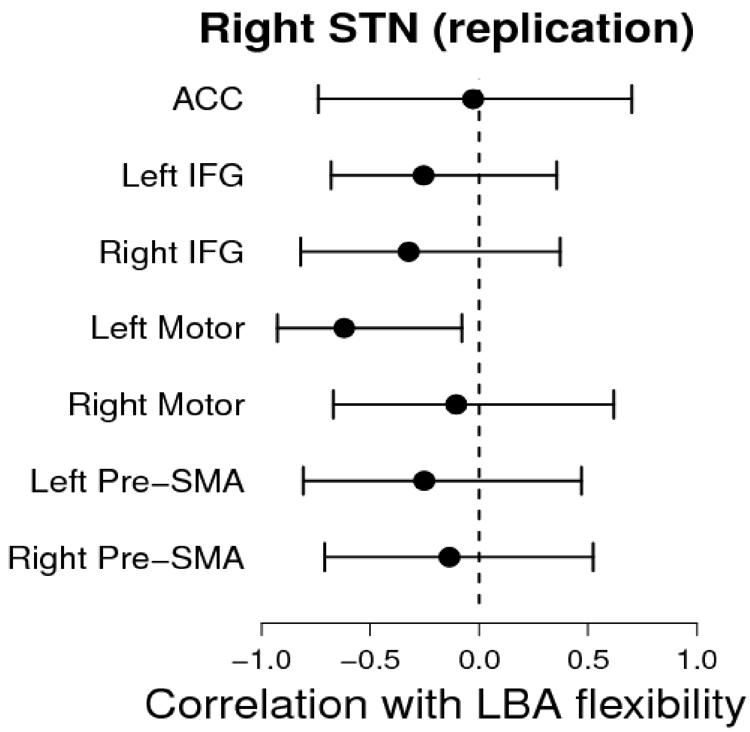

Figure S7. Correlation between LBA flexibility (i.e., the difference in the LBA caution parameter between accuracy and speed conditions) and tract strength from right STN to select brain areas (for the replication study). ACC = anterior cingulate cortex, IFG = inferior frontal gyrus (BA 44), pre-SMA = pre-supplementary motor cortex. Error bars indicate 95% confidence intervals.

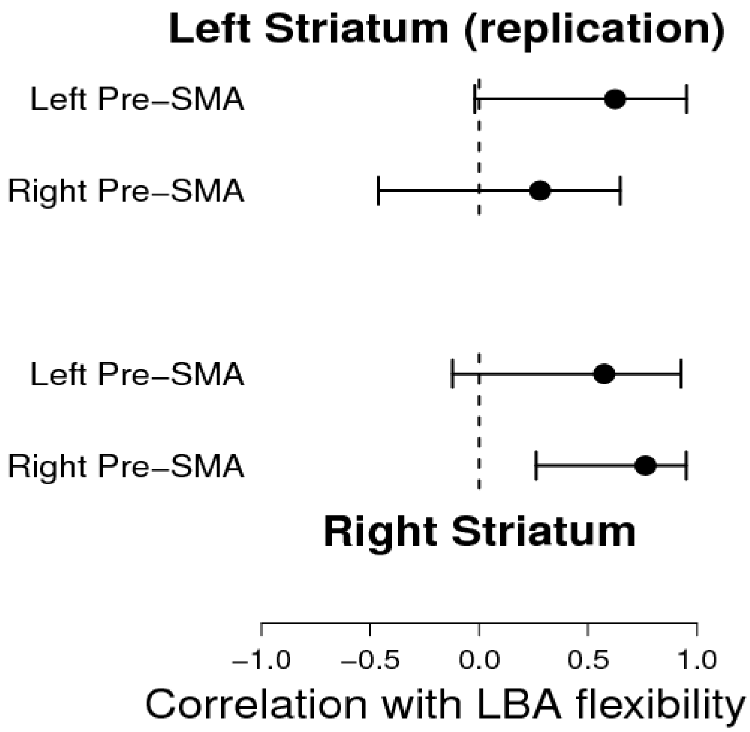

Figure S8. Correlation between LBA flexibility (i.e., the difference in the LBA caution parameter between accuracy and speed conditions) and tract strength from left and right striatum to left and right pre-SMA (for the replication study). Error bars indicate 95% confidence intervals.

Region	Mean (SD)
Left Pre-SMA	0.935 (0.040)
Right Pre-SMA	0.845 (0.062)

Table S1. Mean and standard deviation of tracts that connect to the left striatum. Pre-SMA=Pre-supplementary motor cortex.

Region	Mean (SD)
Left Pre-SMA	0.867 (0.081)

Table S2. Mean and standard deviation of tracts that connect to the right striatum. Pre-SMA=Pre-supplementary motor cortex.

Region	Mean (SD)
Left IFG	0.261 (0.085)
Right IFG	0.073 (0.026)
ACC	0.134 (0.043)
Left motor	0.210 (0.031)
Right motor	0.055 (0.015)
Right Pre-SMA	0.309 (0.042)
Left Pre-SMA	0.329 (0.110)

Table S3. Mean and standard deviation of tracts that connect to the left STN. IFG=Inferior frontal gyrus (BA 44), ACC=Anterior cingulate cortex, Pre-SMA=Pre-supplementary motor cortex.

Region	Mean (SD)
Left IFG	0.061 (0.030)
Right IFG	0.226 (0.112)
ACC	0.164 (0.056)
Left motor	0.062 (0.019)
Right motor	0.168 (0.027)
Right Pre-SMA	0.327 (0.054)
Left Pre-SMA	0.302 (0.062)

Table S4. Mean and standard deviation of tracts that connect to the right STN. IFG=Inferior frontal gyrus (BA 44), ACC=Anterior cingulate cortex, Pre-SMA=Pre-supplementary motor cortex.

Region	Mean (SD)
Left Pre-SMA	0.816 (0.129)
Right Pre-SMA	0.786 (0.122)

Table S5. Replication study. Mean and standard deviation of tracts that connect to the left striatum.

Region	Mean (SD)
Left Pre-SMA	0.773 (0.193)

Table S6. Replication study. Mean and standard deviation of tracts that connect to the right striatum.

Region	Mean (SD)
Left IFG	0.275 (0.062)
Right IFG	0.259 (0.069)
ACC	0.088 (0.049)
Left motor	0.263 (0.090)
Right motor	0.080 (0.057)
Right Pre-SMA	0.261 (0.053)
Left Pre-SMA	0.271 (0.134)

Table S7. Replication study. Mean and standard deviation of tracts that connect to the left STN. IFG=Inferior frontal gyrus (BA 44), ACC=Anterior cingulate cortex.

Region	Mean (SD)
Left IFG	0.022 (0.025)
Right IFG	0.410 (0.178)
ACC	0.153 (0.065)
Left motor	0.031 (0.017)
Right motor	0.184 (0.084)
Right Pre-SMA	0.220 (0.115)
Left Pre-SMA	0.318 (0.168)

Table S8. Replication study. Mean and standard deviation of tracts that connect to the right STN.

References

1. Dormont D, Ricciardi KG, Tandé D, Parain K, Menuel C, Galanaud D, Navarro S, Cornu P, Agid Y, Yelnik J (2004) Is the Subthalamic Nucleus Hypointense on T2-Weighted Images? A Correlation Study Using MR Imaging and Stereotactic Atlas Data. *AJNR Am J Neuroradiol* 25: 1516-23.

2. Marani E, Heida T, Lakke EAJF, Usunoff KG (2008) The Subthalamic Nucleus Part I: Development, Cytology, Topography and Connections. Springer Verlag.

3. Shrout PE, Fleiss JL (1979) Intraclass correlations: Uses in assessing rater reliability. *Psychological Bulletin*. 86: 420-428.

4. Cohen J (1960) A coefficient of agreement for nominal scales. *Educational and Psychological Measurement* 20: 37–46.

5. Forstmann BU, Dutilh G, Brown S, Neumann J, von Cramon DY, Ridderinkhof KR, Wagenmakers E-J (2008) Striatum and pre-SMA facilitate decision-making under time pressure. *Proc Natl Acad Sci USA* 105: 17538-17542.

6. Frank MJ (2006) Hold your horses: A dynamic computational role for the subthalamic nucleus in decision making. *Neural Networks* 19: 1120-36.

7. Aron AR, Poldrack RA (2006) Cortical and subcortical contributions to Stop signal response inhibition: role of the subthalamic nucleus. *J Neurosci* 26: 2424-33.

8. Aron AR, Behrens TE, Smith S, Frank MJ, Poldrack RA (2007) Triangulating a cognitive control network using diffusion-weighted magnetic resonance imaging (MRI) and functional MRI. *J Neurosci* 27: 3743-52.

9. Ivanoff J, Branning P, Marois R (2008) fMRI evidence for a dual process account of the speed-accuracy tradeoff in decision-making. *PLoS One* 9: e2635.

10. van Veen V, Krug MK, Carter CS (2008) The neural and computational basis of controlled speed-accuracy tradeoff during task performance. *J Cogn Neurosci* 20: 1952-1965.

11. Alexander GE, Crutcher MD (1990) Functional architecture of basal ganglia circuits: Neural substrates of parallel processing. *Trends Neurosci* 13: 266-71.

12. Ratcliff R (1978) A theory of memory retrieval. Psychol Rev 85:59-108.